

## A Color Segmentation-Based Method to Quantify Atherosclerotic Lesion Compositions with Immunostaining

Congqing Wu, Alan Daugherty, and Hong Lu

### Abstract

There is an increasing recognition that atherosclerotic lesion composition, rather than size, is the determinant of acute events. Immunostaining is a commonly used method to characterize atherosclerotic lesion compositions. Here, we describe a color segmentation-based approach in HSI (hue, saturation, and intensity) color mode, which minimizes subjectivity and produces accurate and consistent quantifications of atherosclerotic lesion compositions.

**Key words** Immunostaining, Atherosclerosis, Antibody, Imaging, Color

---

### 1 Introduction

Mouse models are commonly used to study pathologies and mechanisms of atherosclerosis attributed to the ease of genetic manipulations, availability of large numbers, and cost benefits relative to large species. The two commonly used mouse models, low-density lipoprotein (LDL) receptor  $-/-$  and apolipoprotein E (apoE)  $-/-$  mice, rapidly develop atherosclerosis when fed a saturated fat-enriched diet (generally referred to as “Western diet”) [1–4]. There is also consistent evidence that activation of the renin angiotensin system contributes to hypercholesterolemia-induced atherosclerosis [5–17]. One direct evidence is that infusion of angiotensin II, the major bioactive peptide of the renin angiotensin system, accelerates formation and progression of atherosclerosis in these two hypercholesterolemic mouse models [5, 13, 14]. Conversely, inhibiting key components of the renin angiotensin system reduces atherosclerosis, as demonstrated in both animal models and human trials (a few examples from thousands of publications [8, 10, 12, 15–17]). Therefore, determination of the renin angiotensin components in atherosclerotic lesions may provide mechanistic insights into the development of atherosclerosis.

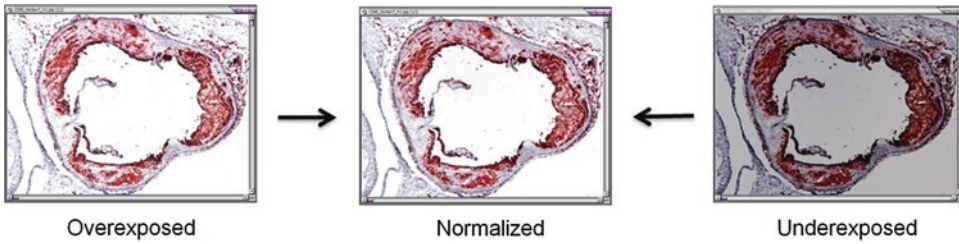


**Fig. 1** Normalization of image background. Overexposed or underexposed images can be normalized to same background by the “Best Fit” mode

Immunostaining detects cell types and molecular markers of the pathologic process at different stages of atherosclerotic lesions. This provides insights into the complexity and dynamic nature of lesion development.

Aortic root is a commonly studied region for atherosclerotic lesions in mouse models. Atherosclerotic lesions in mice are characterized by subendothelial accumulation of leukocytes, of which macrophages are the most abundant cell type with lipid content. A cap develops over these macrophages, which contains smooth muscle cells, is also detected in mouse atherosclerotic lesions. Antibodies that specifically target macrophages (e.g., CD68) and the major resident cell type (smooth muscle cells) of the aortic wall have been well established [18]. Therefore, in Subheading 3 method for quantification of positive immunostaining we will use CD68 (Figs. 1, 2, 3, 4, and 5) and smooth muscle  $\alpha$ -actin (Fig. 5) positive staining as examples.

Here, we also provide insights into chicken antibodies (Table 1) we developed that target mouse angiotensinogen (AGT), renin, or angiotensin-converting enzyme (ACE), as well as antibodies targeting mouse AngII type 1 (AT1) receptors. Chicken antibodies we developed consist of pre-immune IgY (prior to the introduction of antigen from the same hen for the specific antibody), affinity purified chicken anti mouse antibody, and IgY after eluting the specific antibody (depleted IgY). Therefore, this provides two appropriate negative controls for the antibody, pre-immune IgY and depleted IgY. For renin and ACE immunostaining, we have also used tissues from renin and ACE whole body-deficient mice, respectively, as negative controls to validate the specificity of the antibodies to these two respective targets.

To determine whether these renin angiotensin components are present in mouse atherosclerotic lesions, it is important to first validate these antibodies in their major expressing organs. AGT is ubiquitously expressed in many organs. Hepatocytes are the systemic source for AGT [12, 19, 20]. After synthesis, AGT is released to circulating blood, and also redistributed to other organs such as kidney [12, 21, 22]. Therefore, liver, despite being the major source of systemic AGT, is not optimal to validate an AGT antibody. Instead,

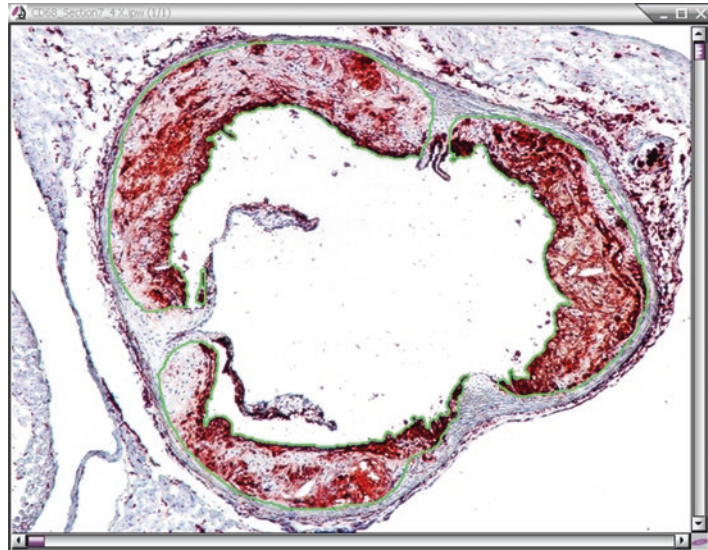


**Fig. 2** Defining area of interest. Atherosclerotic lesions in an aortic root section were visualized with CD68 and hematoxylin staining. Individual lesion areas (within green lines) are manually traced using the “Area” tool bar. Three areas of interest are defined as shown by green outlines

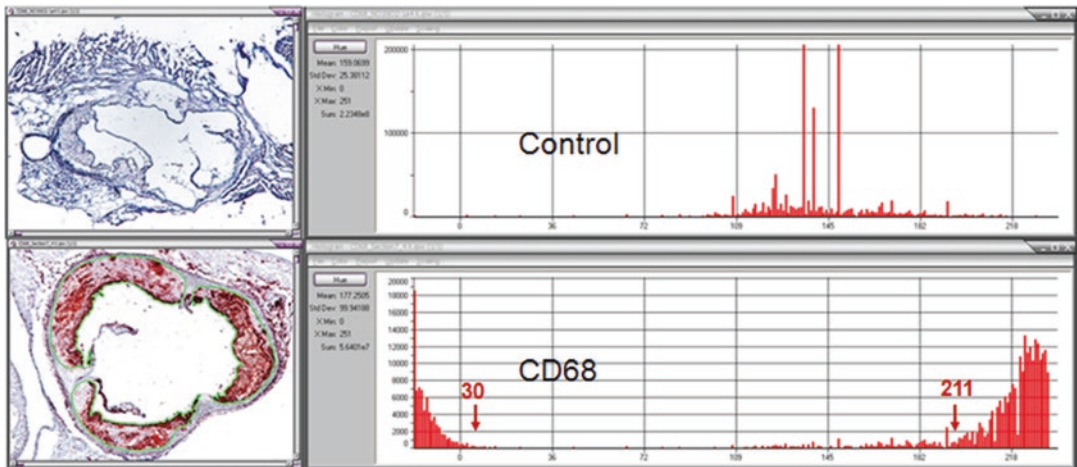


**Fig. 3** Determination of color histogram. HUE channels of the color histogram for CD68 positive immunostaining (red) are defined by comparing to the negative control (non-immune rat IgG2a). Two color segments of HUE (0–30) and (211–255) appearing on CD68 positive staining, but not on the negative control, represent CD68 positive immunostaining

AGT accumulates in proximal convoluted tubules of kidney, which provides an optimal tissue for immunostaining of AGT [22]. In contrast to dispersed expression of AGT in many organs, juxtaglomerular cells (JG) of the kidney are the primary source for renin expression. We have demonstrated that chicken anti mouse renin antibody listed

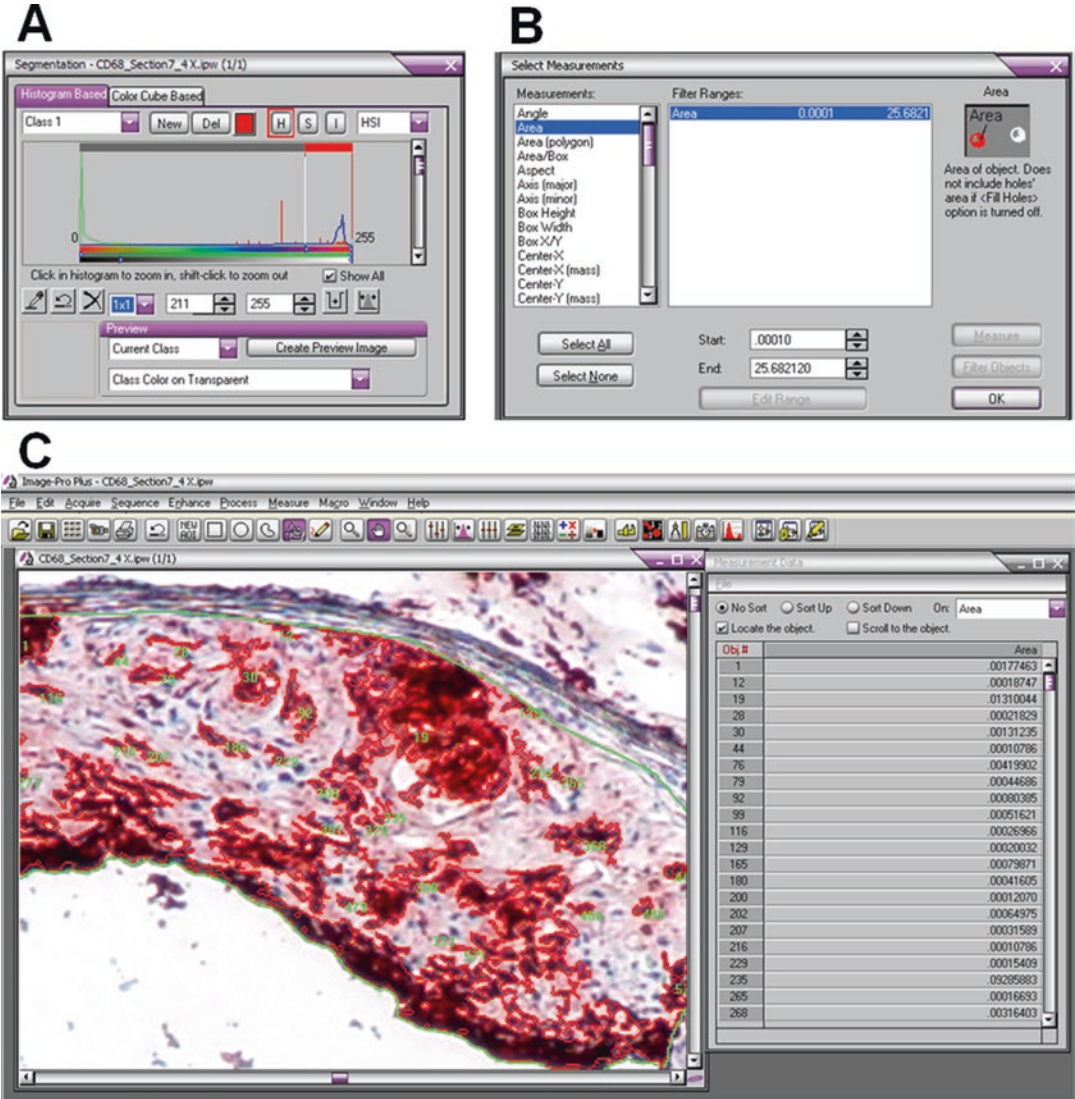


**Fig. 4** Quantification of positive staining. An example for setting up the color segment (A), selecting measurements (B), and automatic calculation of positive staining (C)

in Table 1 only detects renin in kidney JG cells of wild-type, but not renin  $-/-$  mice. ACE is predominantly expressed in vasculature, which is abundant in both endothelial and smooth muscle cells [6, 11, 23]. Therefore, vessels such as the aorta are appropriate tissues for ACE immunostaining. We have demonstrated that chicken anti mouse ACE antibody listed in Table 1 only develops positive staining in wild-type, but not ACE-deficient tissues.

Angiotensin II contributes to atherosclerosis through its interaction with AT1a receptors [6, 7]. There are many commercially available antibodies against mouse AT1 or AT1a receptors. We have



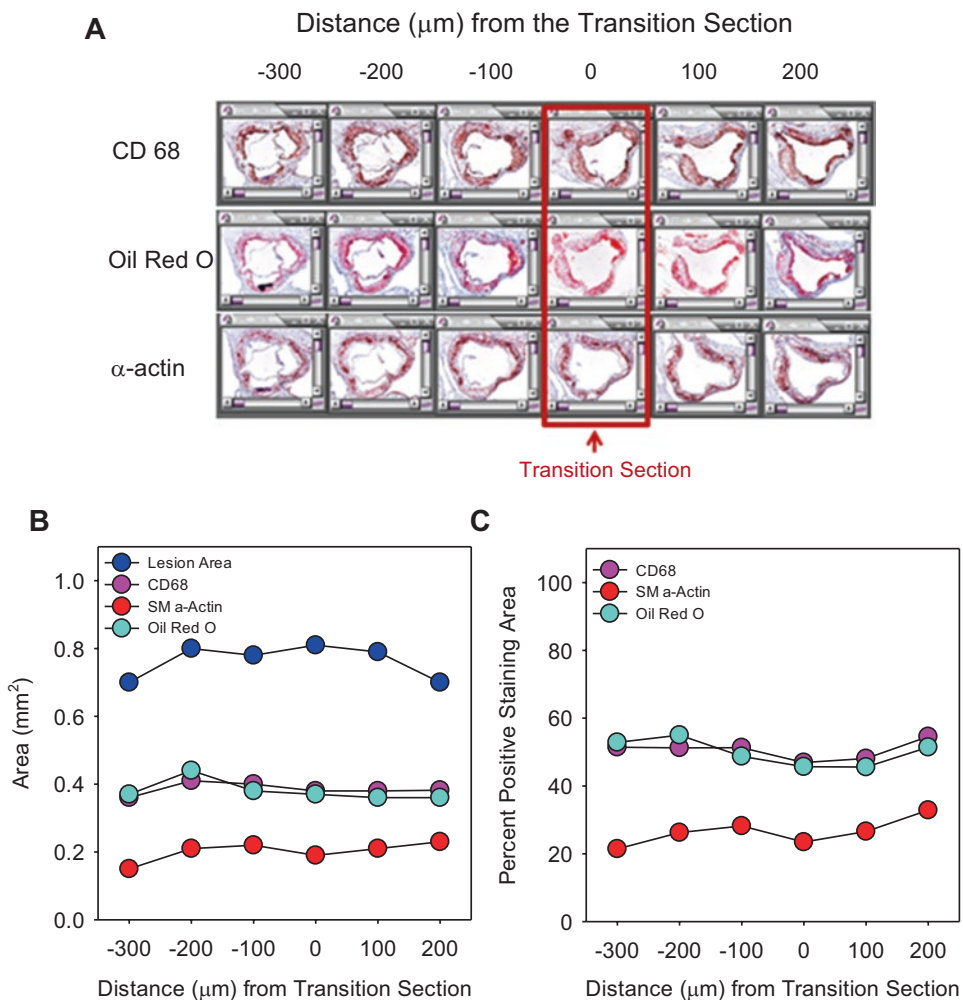


**Fig. 5** Analysis of positive staining in atherosclerotic lesions. A male LDL receptor  $-/-$  mouse was fed “Western diet” for 7 months. **(A)** Images of CD68, oil *red* O, and smooth muscle  $\alpha$ -actin staining (*red* denotes positive staining) throughout the aortic root. “Transition” denotes the ending of the aortic sinus and the beginning of the ascending aorta. **(B)** Positive area of oil *red* O, CD68, and smooth muscle  $\alpha$ -actin. **(C)** Percent positive area is calculated by comparing positive staining area of oil *red* O, CD68, and smooth muscle  $\alpha$ -actin to lesional area (namely, total area of interest)

**Table 1**  
**Chicken anti-mouse IgY antibodies for immunostaining of angiotensinogen, renin, and angiotensin-converting enzyme**

Target	Immunogenic peptide sequence	Recommended positive control tissue	Recommended working concentration	References
AGT	CZEEEQPTTSVQQGSPE	Kidney (proximal convoluted tubules)	10 $\mu\text{g}/\text{ml}$	[6]
Renin	CZRKFYTEFDRHNNR	Kidney (present in JG cells under normal condition)	10 $\mu\text{g}/\text{ml}$	[6, 8]
ACE	CZDLE TDE AKADRFVEEYD RT	Vasculature	3 $\mu\text{g}/\text{ml}$	[6, 11]

AGT angiotensinogen, ACE angiotensin-converting enzyme, JG juxtaglomerular

also developed multiple chicken anti-mouse antibodies targeting different sequences of the AT1a receptor. Consistent with reports from Dr. Saavedra and Dr. Coffman's laboratories [24, 25], we have failed to demonstrate that AT1 receptor can be stained specifically with any antibody in mouse tissues. Therefore, we are not aware of any antibodies that have validated for AT1a receptor immunostaining of mouse atherosclerosis.

Many image analysis programs provide tools to quantify positive staining with RGB color mode (Red, Green, Blue) as their defaulted setting. While it is optimal to select single homogeneous color [26, 27], RGB mode has shortcomings to quantify compositions on complex immunostaining images. It lacks reproducibility since a range of each color channel is arbitrarily selected by the observer. Therefore, it is difficult to define heterogeneous positive staining colors with RGB color mode, which are commonly seen in atherosclerotic lesions. Here, we describe the use of HSI model for color selection. HSI stands for hue (H), saturation (S), and intensity (I) triplet, each component of which can vary from 0 to 255 in 8-bit computing. Hue defines the color itself. For example, red is distinct from blue and yellow. In theory, the values for the hue axis run from 0 to 360°, beginning and ending with red and running through green, blue, and all intermediary colors such as greenish-blue, orange, purple, and other colors. In an image analysis program, 0–360° is converted to 0–255. Saturation denotes the degree to which the hue differs from a neutral gray. Saturation of 0–100% is converted to 0–255. Intensity means the level of illumination. 0% appears black, whereas 100% is full illumination, which washes out color. The 0–100% mode of intensity is also converted to 0–255. HSI matches the manner how we perceive complex color ranges, while remaining computationally simple. Endpoints of color segments representing positive staining are readily determined without personal bias by comparing histograms between a positive staining image and a negative control image in HSI mode. Appropriately applied, this color segmentation-based method is a reliable technique to provide accurate and consistent quantification of positive immunostaining, a useful tool to look into the development of atherosclerosis as well as many other disease processes.

---

## 2 Materials

1. Immunostained cross-sections of aortic root samples.
2. A bright-field microscope with a digital camera for image acquisition.
3. Imaging software that has HSI color mode (Hue, Saturation, Intensity) for quantification of positive immunostaining area and atherosclerotic lesion area.

### 3 Methods

Macrophages are the most abundant cell type in atherosclerotic lesions of hypercholesterolemic mice, whereas smooth muscle cells are the predominant resident cell type of the aortic wall, which also frequently form a boundary (the cap) of atherosclerotic lesions. Lesions are stained with oil red O to determine the amount of neutral lipid. In this Section, we use immunostaining of CD68 (Clone FA-11) and smooth muscle  $\alpha$ -actin as an example to illustrate the Method. Immunostaining of the renin angiotensin components can also be analyzed similarly.

Tissue sections cut on a cryostat were derived from the aortic root of a male LDL receptor $^{-/-}$  mouse fed “Western diet” for 7 months. Sections were stained for neutral lipids with oil red O and immunostained for CD68 (macrophage marker) and smooth muscle  $\alpha$ -actin (smooth muscle cell marker). Images of aortic root sections that were 100  $\mu$ m apart were analyzed using the Image-Pro Plus software. We follow the steps listed below to quantify each image:

1. Image quality control: Make sure all images are taken at same camera settings. Use the “Best Fit” function of the imaging software to fix overexposed or underexposed images (Fig. 1) so that every image has similar background color distribution.
2. Defining area of interest (AOI): Manually trace the whole lesion area as shown in Fig. 2 that green color isolates AOI from the rest of the image. This is to ensure that positive staining is quantified within the defined AOI. Multiple AOIs are allowed. As shown in Fig. 2, three AOIs are defined.
3. Determination of positive immunostaining color range using histogram: Color histogram is a representation of the frequency distribution of colors in an image, determined by counting the number of pixels of each given set of color ranges. This function is under “Measure” in the Image-Pro Plus software. Figure 3 shows the HUE channel of the color histogram of negative control and CD68 positive immunostaining, respectively. Two color segments of HUE (0–30) and (211–255) only appear on CD68 staining but not on its negative control, representing CD68 positive immunostaining. Obtaining these endpoints of color segments using color histogram of the HSI mode is the key to this method (*see Note 1*).
4. Quantification of positive immunostaining: After setting color segments with HUE value (Fig. 4a), select “Measurements” as shown in Fig. 4b. Positive staining area is instantly selected and calculated automatically. Selection of positive immunostaining can be modified by adjusting INTENSITY value. The results are shown as presented in Fig. 4c. Use the same HUE and INTENSITY values for every image of same immunostaining (*see Note 2*).

5. Analysis of lesional composition: There are two methods to analyze data obtained from **step 4**. One is to determine absolute area of lesional composition as shown in Fig. 5b, and the other is to normalize lesional composition to total lesion area as shown in Fig. 5c. There is no standard which method is better. The selection can depend on what content to state. For example, if the user wants to compare whether there are more macrophages accumulated in lesions in one group than the other, the former method is feasible. If the user wants to emphasize whether the ratio of macrophage accumulation in lesions is more in one group than in the other, the latter method is optimal (*see Note 3*).

---

## 4 Notes

1. Specificity of positive immunostaining is a premise for accurate quantification [18]. This is determined by appropriate negative controls including antibody-equivalent immunoglobulin from non-immune or pre-immune same host, exclusion of primary antibody, omission of both primary and secondary antibodies. Availability of tissue sections as a negative control would enhance the reliability of the specificity for immunostaining.
2. Quality of images is the key for accurate measurements using this HSI color segmentation-based method. It is also important to acquire all images using same microscope, same camera setting, and same light conditions.
3. Measuring multiple sections (> 5 serial sections), rather than a single section, enhances the accuracy of quantification. Same as atherosclerotic lesion measurements in a specific region [28, 29], this also requires to use a defined landmark to ensure positive immunostaining in same region is compared.

---

## Acknowledgments

Congqing Wu is supported by an American Heart Association Postdoctoral fellow award (16POST31140008). The authors' research work is supported by an Institutional Development Award from the National Institute of General Medical Sciences of the National Institutes of Health under grant number P20 GM103527 and R01 under grant numbers HL107319 and HL133723 from the National Institutes of Health of the United States of America. The content in this manuscript is solely the responsibility of the authors and does not necessarily represent the official views of the National Institutes of Health.



## References

1. Breslow JL (1996) Mouse models of atherosclerosis. *Science* 272:685–688
2. Ishibashi S, Goldstein JL, Brown MS, Herz J, Burns DK (1994) Massive xanthomatosis and atherosclerosis in cholesterol-fed low density lipoprotein receptor-negative mice. *J Clin Invest* 93:1885–1893
3. Plump AS, Smith JD, Hayek T, Aaltosetala K, Walsh A, Verstuyft JG et al (1992) Severe hypercholesterolemia and atherosclerosis in apolipoprotein-E-deficient mice created by homologous recombination in ES cells. *Cell* 71:343–353
4. Zhang SH, Reddick RL, Piedrahita JA, Maeda N (1992) Spontaneous hypercholesterolemia and arterial lesions in mice lacking apolipoprotein E. *Science* 258:468–471
5. Daugherty A, Manning MW, Cassis LA (2000) Angiotensin II promotes atherosclerotic lesions and aneurysms in apolipoprotein E-deficient mice. *J Clin Invest* 105:1605–1612
6. Daugherty A, Rateri DL, Lu H, Inagami T, Cassis LA (2004) Hypercholesterolemia stimulates angiotensin peptide synthesis and contributes to atherosclerosis through the AT1A receptor. *Circulation* 110:3849–3857
7. Wassmann S, Czech T, van Eickels M, Fleming I, Bohm M, Nickenig G (2004) Inhibition of diet-induced atherosclerosis and endothelial dysfunction in apolipoprotein E/angiotensin II type 1A receptor double-knockout mice. *Circulation* 110:3062–3067
8. Lu H, Rateri DL, Feldman DL, Charnigo RJ Jr, Fukamizu A, Ishida J et al (2008) Renin inhibition reduces hypercholesterolemia-induced atherosclerosis in mice. *J Clin Invest* 118:984–993
9. Daugherty A, Lu H, Rateri DL, Cassis LA (2008) Augmentation of the renin-angiotensin system by hypercholesterolemia promotes vascular diseases. *Future Lipidol* 3:625–636
10. Lu H, Balakrishnan A, Howatt DA, Wu C, Charnigo R, Liao G et al (2012) Comparative effects of different modes of renin angiotensin system inhibition on hypercholesterolaemia-induced atherosclerosis. *Br J Pharmacol* 165:2000–2008
11. Chen XC, Lu H, Zhao M, Tashiro K, Cassis LA, Daugherty A (2013) Angiotensin-converting enzyme promotes atherosclerosis through an angiotensin I to angiotensin II pathway involving leukocytes. *Arterioscler Thromb Vasc Biol* 33:2075–2080
12. Lu H, Wu C, Howatt DA, Balakrishnan A, Moorleggen JJ, Chen X et al (2016) Angiotensinogen exerts effects independent of angiotensin II. *Arterioscler Thromb Vasc Biol* 36:256–265
13. Daugherty A, Cassis L (1999) Chronic angiotensin II infusion promotes atherogenesis in low density lipoprotein receptor -/- mice. *Ann N Y Acad Sci* 892:108–118
14. Weiss D, Kools JJ, Taylor WR (2001) Angiotensin II-induced hypertension accelerates the development of atherosclerosis in apoE-deficient mice. *Circulation* 103:448–454
15. Imanishi T, Tsujioka H, Ikejima H, Kuroi A, Takarada S, Kitabata H et al (2008) Renin inhibitor aliskiren improves impaired nitric oxide bioavailability and protects against atherosclerotic changes. *Hypertension* 52:563–572
16. Yusuf S, Sleight P, Pogue J, Bosch J, Davies R, Dagenais G (2000) Effects of an angiotensin-converting-enzyme inhibitor, ramipril, on cardiovascular events in high-risk patients. The heart outcomes prevention evaluation study investigators. *N Engl J Med* 342:145–153
17. ONTARGET Investigators, Yusuf S, Teo KK, Pogue J, Dyal L, Copland I et al (2008) Telmisartan, ramipril, or both in patients at high risk for vascular events. *N Engl J Med* 358:1547–1559
18. Lu H, Rateri DL, Daugherty A (2007) Immunostaining of mouse atherosclerosis lesions. *Methods Mol Med* 139:77–94
19. Wu C, Xu Y, Lu H, Howatt DA, Balakrishnan A, Moorleggen JJ et al (2015) Cys18-Cys137 disulfide bond in mouse angiotensinogen does not affect AngII-dependent functions in vivo. *Hypertension* 65:800–805
20. Yiannikouris F, Wang Y, Shoemaker R, Larian N, Thompson J, English VL et al (2015) Deficiency of angiotensinogen in hepatocytes markedly decreases blood pressure in lean and obese male mice. *Hypertension* 66:836–842
21. Wu C, Lu H, Cassis LA, Daugherty A (2011) Molecular and pathophysiological features of angiotensinogen: a mini review. *N Am J Med Sci (Boston)* 4:183–190
22. Matsusaka T, Niimura F, Shimizu A, Pastan I, Saito A, Kobori H et al (2012) Liver angiotensinogen is the primary source of renal angiotensin II. *J Am Soc Nephrol* 23:1181–1189
23. Chen XC, Howatt DA, Balakrishnan A, Moorleggen JJ, Wu CQ, Cassis LA et al (2016) Angiotensin-converting enzyme in smooth muscle cells promotes atherosclerosis. *Arterioscler Thromb Vasc Biol* 36:1085–1089
24. Benicky J, Hafko R, Sanchez-Lemus E, Aguilera G, Saavedra JM (2012) Six commercially available

- angiotensin II AT(1) receptor antibodies are non-specific. *Cell Mol Neurobiol* 32:1353–1365
25. Herrera M, Sparks MA, Alfonso-Pecchio AR, Harrison-Bernard LM, Coffman TM (2013) Response to lack of specificity of commercial antibodies leads to misidentification of angiotensin type-1 receptor protein. *Hypertension* 61:e32
  26. Zhang G, Chen Y, BilalWaqar A, Han L, Jia M, Xu C et al (2015) Quantitative analysis of rabbit coronary atherosclerosis. Practical techniques utilizing open-source software. *Anal Quant Cytol Histol* 37:115–122
  27. Vrekoussis T, Chaniotis V, Navrozoglou I, Dousias V, Pavlakis K, Stathopoulos EN et al (2009) Image analysis of breast cancer immunohistochemistry-stained sections using ImageJ: an RGB-based model. *Anticancer Res* 29:4995–4998
  28. Daugherty A, Whitman SC (2003) Quantification of atherosclerosis in mice. *Methods Mol Biol* 209:293–309
  29. Daugherty A, Lu H, Howatt DA, Rateri DL (2009) Modes of defining atherosclerosis in mouse models: relative merits and evolving standards. *Methods Mol Biol* 573:1–15

The Renin-Angiotensin-Aldosterone System

Methods and Protocols

Thatcher, S.E. (Ed.)

2017, X, 201 p. 58 illus., 38 illus. in color., Hardcover

ISBN: 978-1-4939-7028-5

A product of Humana Press